Mon. Not. R. Astron. Soc. **000**, 000–000 (0000) Printed 4 January 2018 (MN LATEX style file v2.2)

# Physical sizes of Mg II haloes beyond $z = 5$: a statistical study

Sarah E. I. Bosman[1], Alex Codoreanu[2]

**ABSTRACT**

## 1 INTRODUCTION

Metal enrichment in the circum- and meta-galactic medium is a leading probe of galaxy evolution. At low and intermediate redshifts, the composition of metal-enriched gas studied in the emission and absorption has yielded unique insight into the nature of galactic inflows and outflows. However, metal enrichment at high redshift currently poses both a theoretical and observational challenge.

There are a few reasons why the exploration of metal enrichment at $z > 5$ is increasingly complicated. First, the huge distances involved, coupled with lower metallicities at early times, mean that emission from excited ions is unresolved with current instruments unless lensing is involved. At the same time, the sparsity of bright background sources seriously limits the study of transverse detections of metal-enriched regions. Without the details of gaseous multi-phase processes which are visible in low-redshift galaxies, the trends observed in occurrence statistics of high-redshift metals remain sparse and puzzling.

On tracer of enrichment which has been studied consistently across redshift is the occurrence of the Mg II $\lambda\lambda$2796.3542 2803.5314Å doublet along quasar lines of sight. This feature is a widely used tracer of cool, ionised gas, associated with various properties of star-forming galaxies (e.g. Churchill et al. 1999, 2013; Ménard & Chelouche 2009; Weiner et al. 2009; Chen et al. 2010; Kacprzak et al. 2011; Matejek & Simcoe 2012). The transition has been used to probe the properties of low-luminosity galaxies, intra-cluster gas, and $L_*$ galaxies (Churchill et al. 1999; Gauthier 2013; Bergeron & Boissé 1991; Steidel et al. 1994).

Paragraph on observational studies

Paragraph on numerical studies

In this letter, we aim to use a simple analytical model to convert lines-of-sight occurrence statistics of Mg II absorption into constraints on the sizes of Mg II -enriched haloes around galaxies ($R$) at $7 > z > 5$. We present the full range of $R(M_{AB})$ relations presently allowed by the observations. This formulation of current observations will be of use to numerical modellers wishing to resolve metal enrichment effects beyond $z = 5$, as well as observers looking for the elusive transverse metal enrichment at those redshifts.

Paragraph on structure of paper

## 2 ANALYTICAL MODEL

The following derivation, first outlined in Steidel (1995), offers a way to link the number density of absorbers ($dN/dX$ or $dN/dz$) to the radius of enriched regions, given known relations for the luminosity function (LF, $\Phi(L)$) and a form of the $R$-luminosity relation. The number of absorbers per absorption path-length is given by

$$\frac{dN}{dX} = \frac{c\sigma n}{H_0} \tag{1}$$

where the 'gas cross-section' $n\sigma$ is given by

$$n\sigma = \pi \int_{L_{\rm min}}^{\infty} f_R(L)\Phi(L)R^2(L)dL, \tag{2}$$

and the pathlength $X$ is defined as

$$\frac{dX}{dz} = (1+z)^2 \frac{H_0}{H(z)} \tag{3}$$

.

The luminosity function $\Phi(L)$ has empirically been determined to be well described by a Schechter function down to magnitudes $M_{AB} \leqslant -15.0$:

$$\Phi(L)dL = \Phi^*(L/L^*)^{\alpha}\exp(-L/L^*)dL. \tag{4}$$

The LF is determined by two parameters $\Phi^*, \alpha$. At $5 < z < 7$, the determinations of these parameters by various authors are mildly discrepant, mostly due to systematic uncertainties (Bouwens et al. 2016). since our aim is to determine the range of enrichment radii permitted by observations, we include all current measurements of $\Phi^*, \alpha$ in our error budget. The range of values used herein are displayed in Table X.

The scaling of enrichment radius with galaxy luminosity has been successfully modelled at low redshift by a Holmberg-like power-law (Bergeron & Boissé 1991),

$$R(L) = R^*(L/L^*)^{\beta}. \tag{5}$$

This relation is remarkably tight at low redshift, for instance, Nielsen et al. (2013) find $\beta = 0.23 \pm 0.01$ for a population of 182 absorber-galaxy pairs at $0.072 \leqslant z \leqslant 1.120$. However, the size of ionised regions is set by the luminosities of host galaxies and the strength of the ultra-violet background (UVB), at least one of which is known to be changing rapidly at the end of hydrogen reionisation (e.g. Stark et al. 2010; Forero-Romero et al. 2012). It is therefore highly

unclear how $R(L)$ should evolve with redshift, and we decide to use the full range of $\beta = [0.1, 0.5]$ with a flat prior to reflect the uncertainty. Throughout the paper we use a pivot $L^* = 9.61 \cdot 10^{36}$ erg s$^{-1}$, corresponding to to $M^*_{AB} = -21.2$.

Grouping expressions (5) and (4) into (2), we obtain,

$$\begin{aligned} n\sigma &= \pi \int_{L_{\rm min}}^{\infty} \Phi^* {R^*}^2 (L/L^*)^{\alpha+2\beta} \exp(-L/L^*) dL \\ &= \pi \Phi^* {R^*}^2 \Gamma(\alpha + 2\beta + 1, L_{\rm min}/L^*) \end{aligned} \quad (6)$$

Where $\Gamma$ is the upper incomplete gamma function, and $L_{\rm min}$ is the limiting magnitude of enriched galaxies. Note that by construction, $L_{\rm min}$ is the magnitude of the faintest galaxies for which Mg II is detectable, i.e., $W_{\rm rest} \geqslant 0.1$Å.

Finally, using (1) we obtain,

$$\frac{dN}{dX} = f_R(L) \frac{c\pi}{H_0} \Phi^* {R^*}^2 \Gamma(\alpha + 2\beta + 1, L_{\rm min}/L^*), \quad (7)$$

or equivalently,

$$R^2 = \frac{H_0}{c\pi} f^{-1} \left( \frac{L}{L^*} \right)^{2\beta} \frac{dN}{dX} {\phi^*}^{-1} \Gamma^{-1} \left( \alpha + 2\beta + 1, L_{min}/L^* \right). \quad (8)$$

Tables 1 and 2 show the most current constraints on $\alpha, \Phi^*$ and $dN/dX$, which we will use in the next section. While measurements of $\alpha$ over $5 \leqslant z \leqslant 7$ are consistent among all published studies within error, this is not the case for the other luminosity function parameter $\Phi^*$. Much debate is ongoing regarding this topic, with the leading proposed source of systematics being a mis-estimation of the lensing model uncertainties. We are not concerned in this paper with obtaining the most precise value of $\Phi^*$, but simply exploring all models allowed within observational constraints. We therefore adopt the maximally conservative approach of an 'allowed range' for $\Phi^*$ extending from the one-sigma lowest allowed value by any author, to the highest one-sigma allowed value by any author in the recent literature. This yields bounds of $\Phi^* \in [0.0007, 0.001]$ at $z = 5.0$, $\Phi^* \in [0.0001, 0.00028]$ at $z = 6.0$, and $\Phi^* \in [0.000062, 0.00079]$ at $z = 7.0$.

Table 3 gives the allowed parameter ranges for $\beta, f$ and $L_{\rm min}/L^*$, which have not been measured directly at these redshifts. Values of $\beta = 0.23 \pm 0.01$ and $f = 0.84 \pm 0.04$ have been measured by Nielsen et al. (2013) at $0.072 < z < 1.120$, but these values are expected to be different in the early universe as galaxy formation is ongoing, the UVB is patchier, and metal enrichment has not reached present-day levels. The value of $L_textmin$, the limiting luminosity above which galaxies contain Mg II , is even more unconstrained and we accordingly treat it as a free parameter.

## 3 RESULTS AND DISCUSSION

which means that for each value of $L_{min}$, it is always possible to find a value of $\beta$ which reproduces the observations. Doing things this way, we can input the measurements of dN/dX (with uncertainties) and deduce $R^*$ as a function of $\beta$ and $L_{min}$. The results at $z = 5$ are shown in Fig 2.

There are still a wide range of physical conclusions to be drawn without priors. For instance, the size of the *smallest enriched regions*, $R_{min} = R^*(L_{min}/L^*)^{\beta}$, is (surprisingly) stable to varying $\beta$ as shown in Fig 3. This is a useful plot for theorists who run simulations: given a choice of halo mass enrichment threshold, it tells the sizes which the simulations should resolve.

Finally, and in my opinion the most useful aspect of this, is the bottom line of $R(L)$. The relation $R = R^*(L/L^*)^{\beta}$ actually only depends on two parameters: $L_{min}$ and $\beta$, with $R^*$ being obtainable by using our measurements of $dN/dX$. This results in Figure 4, a good summary of all the constraints currently available at $z = 5$ with no priors. The figure really shows how good the constraints already are on the sizes of enriched haloes around faint objects: even 1 detection of a halo larger than these limits would raise very serious problems. It also presents an honest perspective on how uncertain the predictions are for the brightest objects. This figure will be extremely useful to observers looking for associated metal absorbers at high redshift.

| | $\alpha$ | $\phi^*$ | source |
|---|---|---|---|
| $z = 5$ | $-1.75 \pm 0.13$ | $0.000758^{+0.00056}_{-0.00022}$ | Mason et al. (2015) |
| | $-1.76 \pm 0.06$ | $0.00079^{+0.00023}_{-0.00018}$ | Bouwens et al. (2015) |
| | $-1.67^{+0.05}_{-0.06}$ | $0.000895^{+0.000192}_{-0.000131}$ | Finkelstein et al. (2015) |
| $z = 6$ | $-2.10^{+0.08}_{-0.03}$ | $0.00023 \pm 0.00002$ | Livermore et al. (2017) |
| | $-2.02^{+0.10}_{-0.10}$ | $0.000186^{+0.000094}_{-0.000080}$ | Finkelstein et al. (2015) |
| $z = 7$ | $-2.07^{+0.05}_{-0.04}$ | $0.00021 \pm 0.00002$ | Livermore et al. (2017) |
| | $-2.04^{+0.17}_{-0.13}$ | $0.00028^{+0.00051}_{-0.00018}$ | Atek et al. (2015) |
| | $-1.94^{+0.09}_{-0.11}$ | $0.00050^{+0.00013}_{-0.00018}$ | Ishigaki et al. (2015) |
| | $-2.03^{+0.21}_{-0.20}$ | $0.000157^{+0.000149}_{-0.000095}$ | Finkelstein et al. (2015) |

**Table 1.** Current measurements of the UV LF parameters $\alpha$ and $\Phi^*$ from various recent studies. The mild discrepancies are most likely due to systematic differences between measurement techniques.

| | $dN/dX$ | source |
|---|---|---|
| $z = 5$ | $0.86 \pm 0.19$ | Codoreanu et al. (2017) |
| $z = 6.5$ | $1.00^{+0.75}_{-0.5}$ | Bosman et al. (2017) |

**Table 2.** Current measurements of occurrence rates of Mg II absorption. The measurements are sensitive to systems with $W_{\rm rest} \geqslant 0.1$Å. Value from Bosman et al. (2017) incorporates the data from Chen et al. (2016) over the same range.

## 4 TODO

(i) Do other redshift ranges

## 5 CONCLUSIONS

## REFERENCES

Atek, H., Richard, J., Kneib, J.-P., et al. 2015, ApJ, 800, 18

| $\beta$ | $f$ | $L_{\rm min}/L^*$ |
|---|---|---|
| $[0.1 - 0.5]$ | $[0.5 - 1.0]$ | $[0.0001 - 1.0]$ |

**Table 3.** Allowed ranges for parameters which have not been directly measured at $z > 5$.

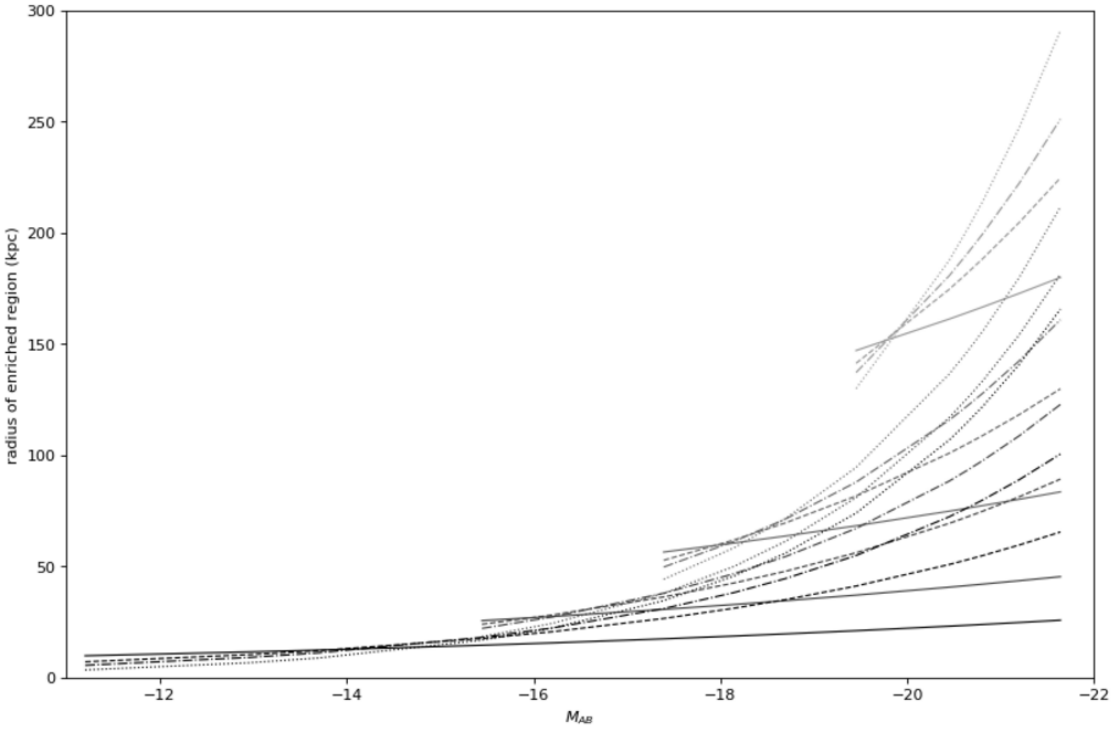


**Figure 1.** Relation between an object's AB magnitude and the expected size of the surrounding Mg II enriched region. Shades of grey correspond to varying $L_{min}/L^* = 0.0001, 0.001, 0.01, 0.1$ corresponding to limiting magnitudes of $M_{min} = -11.2, -13.7, -16.2, -18.7$, from dark to light. Line shape shows the effect of varying $\beta = 0.1, 0.23, 0.3, 0.4$, from continuous to dashed to dotted. Not all lines extend to low luminosities, since those systems are not enriched if $M_{min}$ is high.

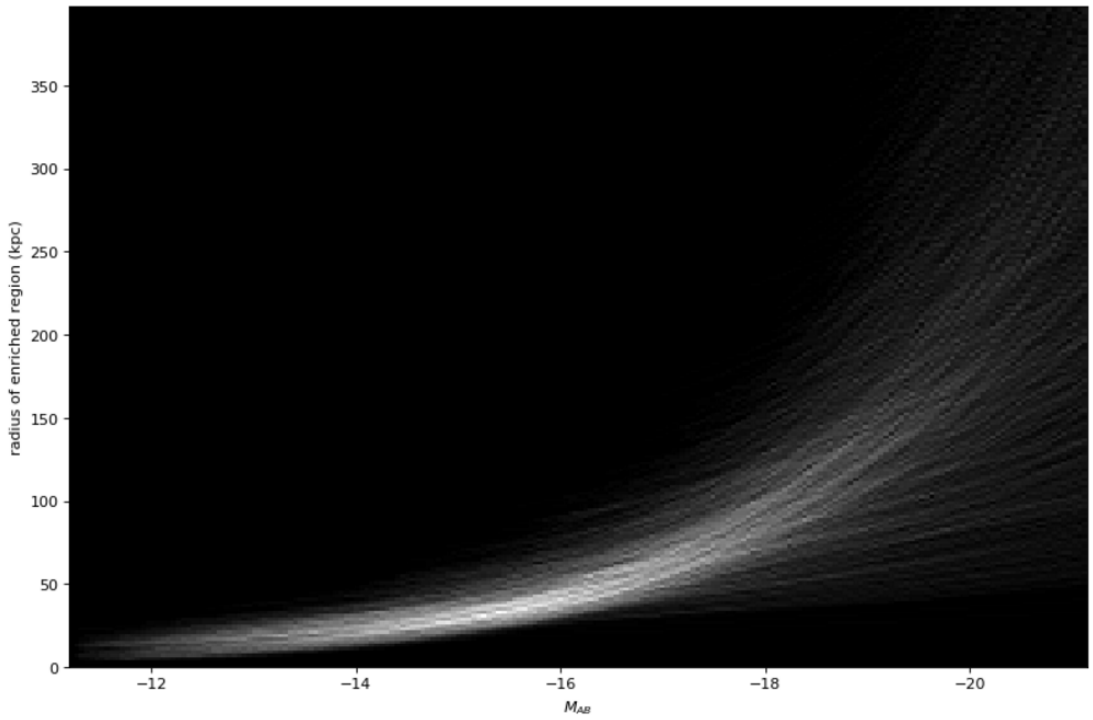


**Figure 2.** Same as Figure 1 for a continuum of models, with all parameters in equation (8) sampled from the allowed ranges given in Tables 1,2 and 3. The regions through which the largest number of models pass are shown in lighter gray, but depend strongly on the choice of prior used for sampling $L_{\rm min}$ (and to a lesser extend $\Phi^*$). This figure showcases the full range of models which are consistent with observations, as opposed to establishing which are more likely. However, some models can be excluded based on negative detections of galaxy-absorber pairs towards quasars as discussed in the text.

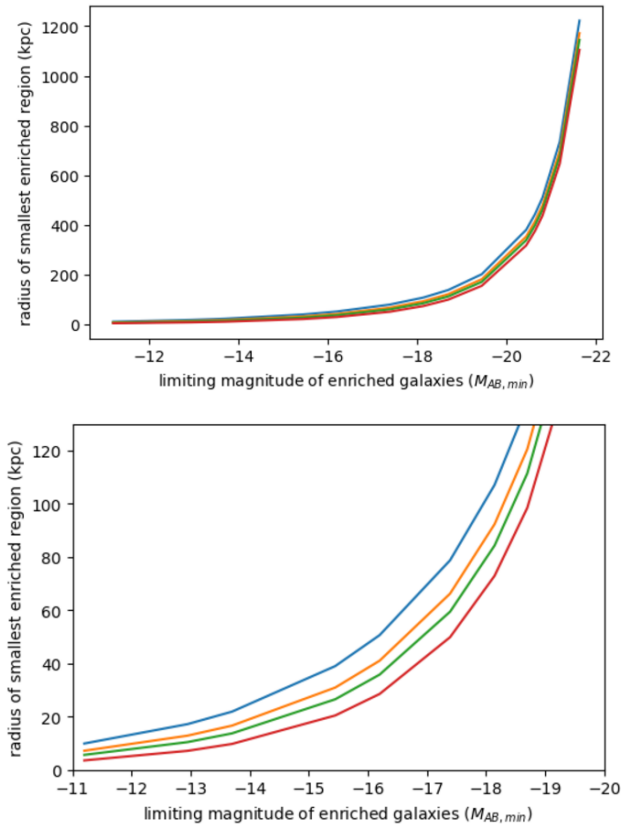


**Figure 3.** Sizes of the smallest enriched haloes: colors blue to red show $\beta = 0.1, 0.23, 0.3, 0.4$. Bottom is a zoom on the top panel.

Bergeron, J., & Boissé, P. 1991, A&A, 243, 344
Bosman, S. E. I., Becker, G. D., Haehnelt, M. G., et al. 2017, MNRAS, 470, 1919
Bouwens, R. J., Oesch, P. A., Illingworth, G. D., Ellis, R. S., & Stefanon, M. 2016, ArXiv e-prints, arXiv:1610.00283
Bouwens, R. J., Illingworth, G. D., Oesch, P. A., et al. 2015, ApJ, 803, 34
Chen, H.-W., Wild, V., Tinker, J. L., et al. 2010, ApJ, 724, L176
Chen, S.-F. S., Simcoe, R. A., Torrey, P., et al. 2016, ArXiv e-prints, arXiv:1612.02829
Churchill, C. W., Nielsen, N. M., Kacprzak, G., & Trujillo, S. 2013, in American Astronomical Society Meeting Abstracts, Vol. 221, American Astronomical Society Meeting Abstracts #221, 227.04
Churchill, C. W., Rigby, J. R., Charlton, J. C., & Vogt, S. S. 1999, ApJS, 120, 51
Codoreanu, A., Ryan-Weber, E. V., Crighton, N. H. M., et al. 2017, ArXiv e-prints, arXiv:1708.00304
Finkelstein, S. L., Ryan, Jr., R. E., Papovich, C., et al. 2015, ApJ, 810, 71
Forero-Romero, J. E., Yepes, G., Gottlöber, S., & Prada, F. 2012, MNRAS, 419, 952
Gauthier, J.-R. 2013, MNRAS, 432, 1444
Ishigaki, M., Kawamata, R., Ouchi, M., et al. 2015, ApJ, 799, 12
Kacprzak, G. G., Churchill, C. W., Barton, E. J., & Cooke, J. 2011, ApJ, 733, 105
Livermore, R. C., Finkelstein, S. L., & Lotz, J. M. 2017, ApJ, 835, 113
Mason, C. A., Trenti, M., & Treu, T. 2015, ApJ, 813, 21
Matejek, M. S., & Simcoe, R. A. 2012, ApJ, 761, 112
Ménard, B., & Chelouche, D. 2009, MNRAS, 393, 808
Nielsen, N. M., Churchill, C. W., & Kacprzak, G. G. 2013, ApJ, 776, 115
Stark, D. P., Ellis, R. S., Chiu, K., Ouchi, M., & Bunker, A. 2010, MNRAS, 408, 1628
Steidel, C. C. 1995, in QSO Absorption Lines, ed. G. Meylan, 139
Steidel, C. C., Dickinson, M., & Persson, S. E. 1994, ApJ, 437, L75
Weiner, B. J., Coil, A. L., Prochaska, J. X., et al. 2009, ApJ, 692, 187